Article

Charge Separation and Catalytic Activity of Ag@TiO Core–Shell Composite Clusters under UV–Irradiation

Tsutomu Hirakawa, and Prashant V. Kamat

J. Am. Chem. Soc., **2005**, 127 (11), 3928-3934• DOI: 10.1021/ja042925a • Publication Date (Web): 23 February 2005

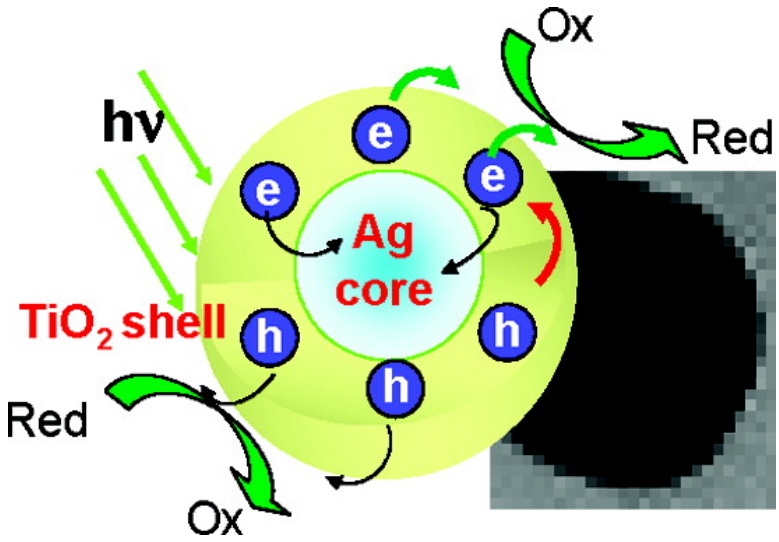

More About This Article

Additional resources and features associated with this article are available within the HTML version:

- Supporting Information
- Links to the 26 articles that cite this article, as of the time of this article download
- Access to high resolution figures
- Links to articles and content related to this article
- Copyright permission to reproduce figures and/or text from this article

View the Full Text HTML

J|A|C|S
ARTICLES
Published on Web 02/23/2005

Charge Separation and Catalytic Activity of Ag@TiO_2 Core−Shell Composite Clusters under UV−Irradiation

Tsutomu Hirakawa[†,§] and Prashant V. Kamat*[,†,‡]

Contribution from the Radiation Laboratory and Department of Chemical and Biomolecular Engineering, University of Notre Dame, Notre Dame, Indiana 46556-0579

Received November 23, 2004; E-mail: pkamat@nd.edu

Abstract: Photocatalytic properties of Ag@TiO_2 composite clusters have been investigated using steady state and laser pulse excitations. Photoexcitation of TiO_2 shell results in accumulation of the electrons in the Ag core as evidenced from the shift in the surface plasmon band from 460 to 420 nm. The stored electrons are discharged when an electron acceptor such as O_2, thionine, or C_{60} is introduced into the system. Charge equilibration with redox couple such as $C_{60}/C_{60}^{\bullet-}$ shows the ability of these core shell structures to carry out photocatalytic reduction reactions. The charge separation, charge storage, and interfacial charge-transfer steps that follow excitation of the TiO_2 shell are discussed.

Introduction

Noble metal nanoparticles such as Ag and Au in the nanosize domain (<10 nm) exhibit unusual catalytic, electric, and optical properties.[1−12] For example, Au nanoparticles of 3−8 nm diameter have been shown to tune the catalytic properties of TiO_2.[13−15] In an earlier study, we have shown that metal nanoparticles deposited on TiO_2 nanostructures undergo Fermi level equilibration following the UV-excitation and enhance the efficiency of charge-transfer process.[16,17] In most of the catalytic studies metal nanoparticles are dispersed on an oxide surface (See for example, refs 18−26). Such a catalyst structure, though effective, result in exposing both metal to reactants and the surrounding medium. Corrosion or dissolution of the noble metal particles during the operation of a photocatalytic reaction is likely to limit the use of noble metal such as Ag and Au.[27−29] A better synthetic design can significantly improve the catalytic performance of oxide-metal composite. Silica has been widely employed as a shell to protect Ag and Au nanoparticles and stabilize them against chemical corrosion. Preparation and characterization of Au@SiO_2 and Ag@SiO_2 core−shell cluster have been reported for metal coreoxide shell clusters.[30−35]

Significant advances have been made in recent years to design metal core-semiconductor shell clusters.[30−32,36−39] Yet, the efforts to utilize these core−shell structures as photocatalysts in the light energy conversion systems (e.g., photoelectrochemical cells, hydrogen production etc.) are limited. In this context, it is important to elucidate the influence of the metal core on the photocatalytic properties of outer TiO_2 shell (Scheme 1). The obvious questions that need to be addressed include, how does the photoinduced charge separation in TiO_2 is influenced

[†] Radiation Laboratory.
[‡] Department of Chemical and Biomolecular Engineering.
[§] Present Address: National Institute of Advanced Industrial Science and Technology (AIST), Tsukuba, Japan.

(1) Henglein, A. *Chem. Rev.* **1989**, *89*, 1861.
(2) Mulvaney, P. *Langmuir* **1996**, *12*, 788.
(3) Pileni, M. P. *New J. Chem.* **1998**, 693.
(4) Templeton, A. C.; Wuelfing, W. P.; Murray, R. W. *Acc. Chem. Res.* **2000**, *33*, 27.
(5) El-Sayed, M. A. *Acc. Chem. Res.* **2001**, *34*, 257.
(6) Toshima, N.; Yonezawa, T. *New J. Chem.* **1998**, *22*, 1179.
(7) Brust, M.; Kiely, C. *Colloid Surf. A* **2002**, *202*, 175.
(8) Kelly, K. L.; Coronado, E.; Zhao, L. L.; Schatz, G. C. *J. Phys. Chem. B* **2003**, *107*, 668.
(9) Kamat, P. V. *J. Phys. Chem. B* **2002**, *106*, 7729.
(10) Adams, D.; Brus, L.; Chidsey, C. E. D.; Creager, S.; Cruetz, C.; Kagan, C. R.; Kamat, P. V.; Lieberman, M.; Lindsay, S.; Marcus, R. A.; Metzger, R. M.; Michel-Beyerle, M. E.; Miller, J. R.; Newton, M. D.; Rolison, D. R.; Sankey, O.; Schanze, K. S.; Yardley, J.; Zhu, X. *J. Phys. Chem. B* **2003**, *107*, 6668.
(11) Kamat, P. V. *Pure Appl. Chem.* **2002**, *74*, 1693.
(12) George Thomas, K.; Kamat, P. V. *Acc. Chem. Res.* **2003**, *36*, 888.
(13) Haruta, M. *Catal. Today* **1997**, *36*, 153.
(14) Yang, Z. X.; Wu, R. Q.; Goodman, D. W. *Phys. Rev. B* **2000**, *6*, 14066.
(15) Valden, M.; Lai, X.; Goodman, D. W. *Science* **1998**, *281*, 1647.
(16) Jakob, M.; Levanon, H.; Kamat, P. V. *Nano Lett.* **2003**, *3*, 353.
(17) Subramanian, V.; Wolf, E. E.; Kamat, P. V. *J. Am. Chem. Soc.* **2004**, *126*, 4943.
(18) Herrmann, J. M.; Disdier, J.; Pichat, P. *J. Phys. Chem.* **1986**, *90*, 6028.
(19) Anpo, M.; Chiba, K.; Tomonari, M.; Coluccia, S.; Che, M.; Fox, M. A. *Bull. Chem. Soc. Jpn.* **1991**, *64*, 543.
(20) Baba, R.; Konda, R.; Fujishima, A.; Honda, K. *Chem. Lett.* **1986**, *10*.
(21) Tada, H.; Teranishi, K.; Ito, S.; Kobayashi, H.; Kitagawa, S. *Langmuir* **2000**, *16*, 6077.
(22) Ohko, Y.; Tatsuma, T.; Fujishima, A. *J. Phys. Chem. B* **2001**, *105*, 10016.
(23) Dawson, A.; Kamat, P. V. *J. Phys. Chem. B* **2001**, *105*, 960.
(24) Averitt, R. D.; Westcott, S. L.; Oldenburg, S. J.; Lee, T. R.; Halas, N. J. *Langmuir* **1998**, *14*, 5396.
(25) Cozzoli, P. D.; Fanizza, E.; Comparelli, R.; Curri, M. L.; Agostiano, A.; Laub, D. *J. Phys. Chem. B* **2004**, *108*, 9623.
(26) Kamat, P. V.; Flumiani, M.; Dawson, A. *Colloids Surf., A.* **2002**, *202*, 269.
(27) Subramanian, V.; Wolf, E.; Kamat, P. V. *J. Phys. Chem. B* **2001**, *105*, 11439.
(28) Subramanian, V.; Wolf, E. E.; Kamat, P. V. *Langmuir* **2003**, *19*, 469.
(29) Lahiri, D.; Subramanian, V.; T.Shibata; Wolf, E. E.; Bunker, B. A.; Kamat, P. V. *J. Appl. Phys.* **2003**, *93*, 2575.
(30) Liz-Marzan, L. M.; Mulvaney, P. *J. Phys. Chem. B* **2003**, *107*, 7312.
(31) Ung, T.; Liz-Marzan, L. M.; Mulvaney, P. *Langmuir* **1998**, *14*, 3740.
(32) Caruso, F.; Spasova, M.; Saigueirino-Maceira, V.; Liz-Marzan, L. M. *Adv. Mater.* **2001**, *13*, 1090.
(33) Mulvaney, P.; Liz-Marzan, L. M.; Giersig, M.; Ung, T. *J. Mater. Chem.* **2000**, *10*, 1259.
(34) Ung, T.; Liz-Marzan, L. M.; Mulvaney, P. *J. Phys. Chem. B* **1999**, *103*, 6770.
(35) Dick, K.; Dhanasekaran, T.; Zhang, Z.; Meisel, D. *J. Am. Chem. Soc.* **2002**, *124*, 2312.
(36) Zhong, C. J.; Maye, M. M. *Adv. Mater.* **2001**, *13*, 1507.
(37) Hardikar, V.; Matijevic, E. *J. Colloid Interface Sci* **2000**, *221*, 133.
(38) Oldenburg, S. J.; Averitt, R. D.; Westcott, S. L.; Halas, N. J. *Chem. Phys. Lett.* **1998**, *288*, 243.
(39) Oldfield, G.; Ung, T.; Mulvaney, P. *Adv. Mater.* **2000**, *12*, 1519.

10.1021/ja042925a CCC: $30.25

Scheme 1

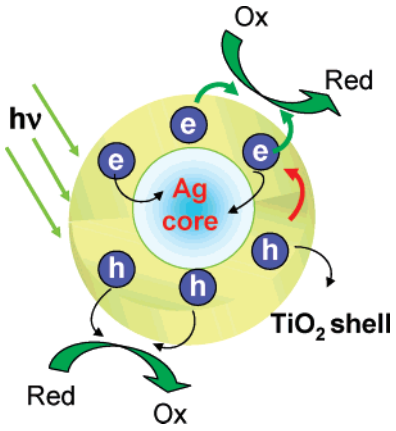

by the metal core? How does the charge equilibration occur between the metal and semiconductor following the band gap excitation? Can these core−shell structures be superior catalysts? To address these questions we have now prepared Ag@TiO_2, Ag@SiO_2, and TiO_2 colloids in DMF/ethanol medium and their behavior under UV-excitation are compared. In a preliminary communication we reported the ability of the Ag@TiO_2 clusters to store electrons under UV-irradiation and discharge them on demand in the dark.[40] The factors that control the charge separation and photocatalytic properties of core−shell nanostructures are presented in this paper. A better understanding of the charge transfer properties is likely to pave the way to develop improved photocatalysts for light energy conversion.

Experimental Section

Materials and Measurements. Titanium-(triethanolaminato) isopropoxide ($N((CH_2)_2O)_3TiOCH(CH_3)_2$) TTEAIP and dimethyl formamide, DMF were purchased from Aldrich. $AgNO_3$ (Fisher ACS grade) was used as received. Active silica ($Na_2O(SiO_2)_{3-5}$, 27 wt % SiO_2) was obtained from Aldrich. Care should be taken to handle toxic solvents such as DMF and hygroscopic materials such as TTEAIP.

The absorption spectra were recorded using UV−vis spectrophotometer (Varian CARY 50 Bio UV−vis Spectrophotometer and SHIMADZU UV-3101 PC UV−vis−NIR Scanning Spectrophotometer). Transmission electron microscopy (TEM) was carried out with JEOL TEM-100SX Electron Microscope and HITACHI H-600 Electron Microscope. Particle size and shape were analyzed with image magnification.

Ag@TiO_2 and Ag@SiO_2 Colloids. For synthesizing Ag@TiO_2 shell cluster, we modified the procedure of reduction of metal ions in dimethylformamide.[41] Desired concentration of TTEAIP (8.3 mM, unless otherwise specified) was prepared in 2-propanol. Two mL of 15 mM $AgNO_3$ solution was mixed with 18 mL of TTEAIP solution. Ten mL of DMF was then added into TTEAIP−Ag solution. The concentration of Ag^+ and TTEAIP in the reaction mixture was 1 mM and 5 mM, respectively. This volume ratio of DMF and *i*-PrOH was optimized by carrying out several batch preparations. When the amount of DMF was too little or when *i*-PrOH was excluded, aggregation of clusters is observed. The volume ratio of DMF and *i*-PrOH hence is an important factor in the preparation of the Ag@TiO_2 clusters. The solution was stirred first for 15 min at room temperature and then refluxed with continued stirring. With continued heating of the solution, the color slowly changed from colorless to light brown. After 90 min, the color of the suspension turned to dark brown. At this point, the heating was stopped and the suspension was stirred until it cooled to room temperature.

Scheme 2

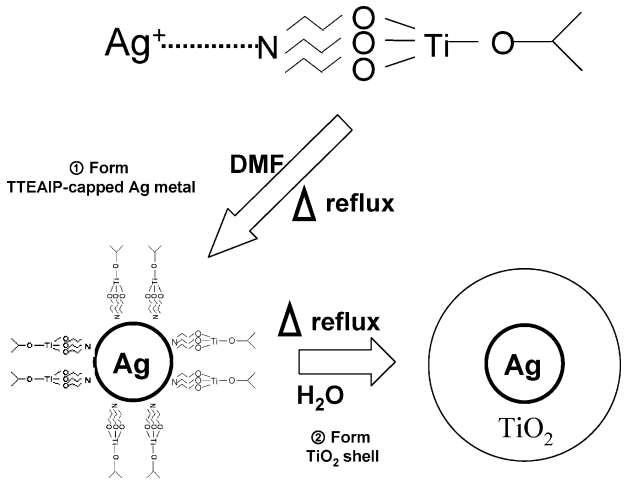

The procedure described above was also employed for preparing silica capped Ag particles (viz., Ag@SiO_2). Active silica was added to the reaction mixture instead of TTAEIP. The details of the method can be found elsewhere.[31] The cluster suspension of Ag@TiO_2 and Ag@SiO_2 was centrifuged and resuspended in ethanol solution. The procedure was repeated at least 3-times to minimize the content of water and DMF in the suspension.

TiO_2 Colloids. TiO_2 colloidal suspension was prepared by the procedure similar to the one used for Ag@TiO_2 colloids except the step of $AgNO_3$ addition. The slow hydrolysis of TTEAIP produced transparent sol of TiO_2.

Laser Flash Photolysis. Experiment of nano-second laser flash photolysis was performed with 308-nm laser pulses from Lambda Physik excimer laser system (Laser pulse width is 10 ns, intensity was ~10 mJ/pulse). Unless otherwise specified, all the experiments were performed under N_2 purging condition.

Steady-state photolysis experiments were conducted by photolyzing N_2-purged solution with UV−visible light (250 W xenon lamp). A $CuSO_4$ filter was introduced in the path of the light beam to cutoff light below the wavelengths of 300 nm.

Results and Discussion

Synthesis of Ag@TiO_2 Cluster Suspension. Metal core-oxide shell structures were prepared by one pot synthesis that involved reduction of metal ions and hydrolysis of Titanium-(triethanolaminato)isopropoxide in dimethylformamide (DMF).[41] The solvent, DMF plays an important role of reducing the Ag^+ ions first, followed by the slow hydrolysis of TTEAIP to form a shell around the metal core. Increasing the amount of DMF increases the primary step of reduction rate of Ag^+ ion to Ag^0. It is important that the reduction rate of Ag^+ ion is greater than the rate of formation of TiO_2 shell. After several initial attempts we have found that the experimental conditions that employ 33% DMF in *i*-PrOH yields stable suspension of core−shell particles. As Ag^+ ions are reduced by DMF to form small metal particles, they quickly interact with the amine groups of TTEAIP. The condensation polymerization of TTEAIP slowly progresses on the surface of Ag particles to yield TiO_2 shell. Formation of core−shell cluster is illustrated in Scheme 2.

The TEM images of two different sets of cluster preparations are presented in Figure 1. The concentrations of TTEAIP in these two sets of synthesis were 0.03 and 5 mM respectively while maintaining the concentration of $AgNO_3$ at 1 mM. In both

(40) Hirakawa, T.; Kamat, P. V. *Langmuir* **2004**, *20*, 5645.
(41) Pastoriza-Santos, I.; Koktysh, D. S.; Mamedov, A. A.; Giersig, M.; Kotov, N. A.; Liz-Marzan, L. M. *Langmuir* **2000**, *16*, 2731.

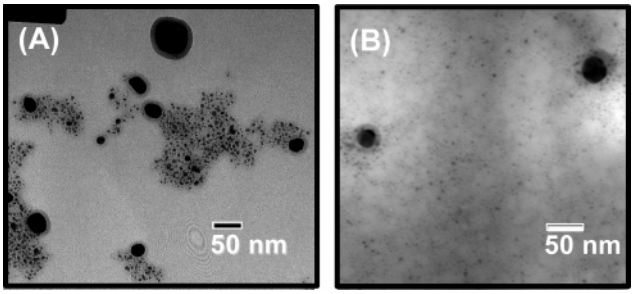

Figure 1. Transmission electron micrographs of Ag@TiO_2 colloids which were prepared using the composition of (A) 5 mM TiO_2 and 1 mM Ag and (B) 5 mM TiO_2 and 1 mM Ag. (C) Absorption spectra of colloidal (a) Ag@TiO_2 (b) Ag@SiO_2 and (c) TiO_2 suspension in ethanol.

cases the Ag core was similar with particle diameter of 3−4 nm. The TEM image shows a majority of dark images of Ag core in this size regime. All these particles have a thin capping of TiO_2 shell of thickness in the range of 1.5−3 nm. The core−shell structure is clearly evident in the few larger fully grown particles (30−65 nm) that coexist with smaller size particles (Figure 1A).

Capping of TiO_2 shell on the Ag core was confirmed by checking the stability in an acidic solution (HNO_3). The Ag cluster, stabilized by citric acid, is readily dissolved in acidic solution (pH = 2). Ag@TiO_2 on the other hand is quite stable in HNO_3 solution even when the TiO_2 shell was thin. If the formation of TiO_2 clusters in DMF was independent such that both clusters are formed separately or in the form of a TiO_2/Ag sandwich structure, we would have observed dissolution of silver clusters. The stability test in acidic solution asserts the argument that the TiO_2 shell on the Ag core is uniform and provides the protection against acid induced corrosion.

One approach to increase the shell thickness is to increase the concentration of the precursor of TiO_2 (TTAEIP in the present case). Similar approach has been widely used for preparing silica capped metal nanoparticles.[31] Thus, for Ag@TiO_2 colloids prepared using higher TTAEIP concentrations we would have expected to see a thicker TiO_2 shell. However, we observe the formation of independent TiO_2 clusters with smaller size Ag@TiO_2 clusters of core diameter of <2 nm (Figure 1B). Unlike silica capped Ag clusters, we cannot grow thicker TiO_2 shell by increasing the concentration of TTAEIP.[42] The hydrolysis of TTEAIP thus, competes with Ag^+ reduction and yields TiO_2 clusters with and without Ag core at high TTEAIP concentration. These results show the necessity for optimizing the concentration of TTEAIP for achieving uniform capping of Ag nanocore.

The particle concentration was estimated by assuming uniform distribution of Ag core particle and an average particle size of 5.12 and 3.65 nm as obtained from Figure 1A and B. The average number of particles in these two preparations were estimated to be 2.4×10^{14} and 6.3×10^{14} per liter, respectively. Figure 2 shows the absorption spectra of Ag@TiO_2, Ag@SiO_2 and TiO_2 colloids before and after UV-irradiation. Ag@SiO_2 and Ag@TiO_2 exhibit strong absorption in the visible. This visible absorption arises from the surface plasmon band of Ag core and it is strongly influenced by the oxide shell. (Where as SiO_2 itself has no absorption in the UV and visible, TiO_2 exhibits

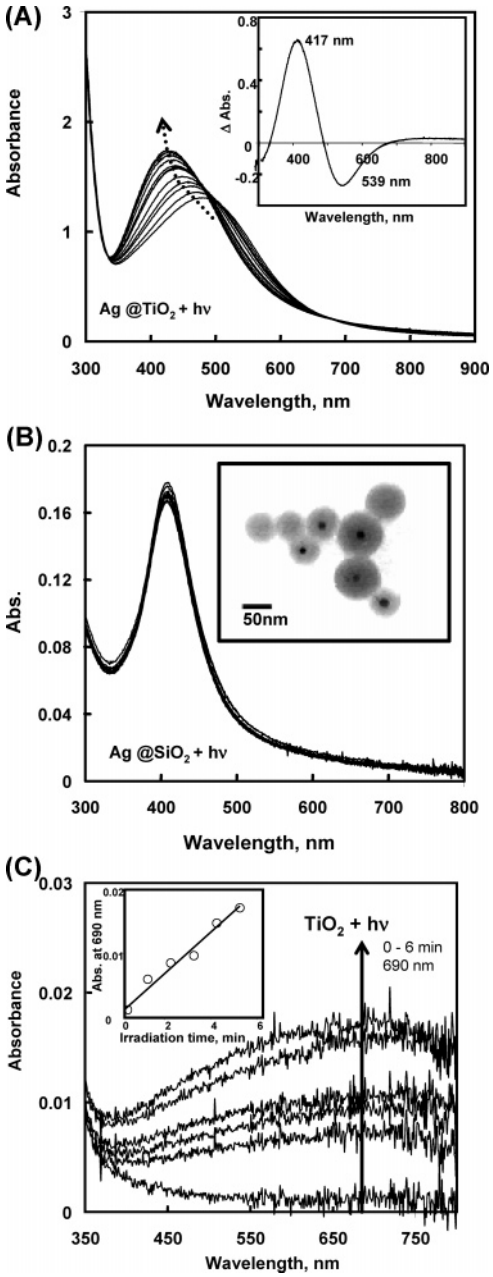

Figure 2. Absorption spectra recorded following UV-irradiation of various colloidal suspensions in ethanol. The direction of the arrow indicates the spectral shift observed during the UV-irradiation. (A) Ag@TiO_2 colloidal suspension. The difference absorption spectrum corresponding to the absorption changes is shown in the inset. (B) Ag@SiO_2 colloidal suspension. The inset shows TEM image of Ag@SiO_2. (C) TiO_2 colloidal suspension. The inset shows the change in absorbance at 690 nm with UV-irradiation.

strong absorption in the UV). The plasmon absorption band of the small Ag particles prepared using borohydride reduction is around 380 nm. The surface plasmon absorption band of Ag@SiO_2 and Ag@TiO_2 particles is significantly red-shifted and the maximum is seen at 410 and 480 nm respectively. It is evident that the red shift in the plasmon absorption seen in the core shell particle is dependent on the type of the oxide shell. As shown earlier,[2,30,41,43] the high dielectric constant of the TiO_2 shell causes a red shift in the plasmon absorption of the silver core.

(42) Faster capping of Ag nuclei by the amine moieties is likely to suppress the growth of Ag nanoparticles at higher TTAEIP concentration

(43) Kreibig, U.; Vollmer, M. *Optical Properties of Metal Clusters*; Springer: Berlin, 1995.

The peak shift is brought about by the refractive index of the surrounding medium. In core−shell structure, the plasmon peak position of the metal core can be related using the expression 1[44]

$$\lambda = \{\lambda_p[\epsilon^\infty + 2n^2_{EtOH} + 2g(n^2_{TiO2} - n^2_{EtOH})/3]\}^{1/2} \quad (1)$$

where n is refractive index of the surrounding medium, ϵ^∞ is high frequency of the core metal, g is the volume fraction of shell layer, λ is the estimated peak position of metal core, and λ_P is bulk plasma wavelength as represented in eq 2

$$\lambda_P = [4\,\pi^2\,c^2\,m_{eff}\,\epsilon_0/N\,e^2]^{1/2} \quad (2)$$

where the m_{eff} is effective mass of the free electron of the metal, and N is electron density of metal core.

For Ag cluster with no medium effect we expect λ_P to be around 136.3 nm. When the Ag cluster was dispersed in water or ethanol the λp is observed around 390 nm. Since n_{TiO2} (2.5) for shell is much higher than n_{EtOH} (1.359), the plasmon absorption shows a large red shift. With increasing thickness of TiO_2 shell the g factor in expression (1) becomes close to unity and the red shift of plasmon absorption attains a maximum value for the Ag@TiO_2 cluster. On the basis of the expression 1, we expect the value of λ to be around 463 nm. In the present experiment, we observe rather broad plasmon absorption with a maximum around 480 nm and this red-shifted maximum is close to the value expected from the theoretical prediction. Factors such as scattering effects and adsorbed chemical species are likely to contribute to the small discrepancy between estimated and experimentally observed plasmon absorption peak.

Steady-State Photolysis. Figure 2A shows the changes in the absorption spectrum following the UV-irradiation of Ag@TiO_2 colloids suspended in deaerated ethanol. Before subjecting the Ag@TiO_2 colloids in ethanol to UV irradiation, the plasmon absorption peak is seen at 480 nm. As these colloids are subjected to UV irradiation we observe a blue shift in the plasmon absorption band. After irradiating with UV-light for ~30 min, the absorption shift attains a plateau with a surface plasmon absorption peak at 420 nm. The shift of 60 nm in the plasmon absorption reflects increased electron density in the Ag core during photoirradiation. Since TiO_2 undergoes charge separation under UV-irradiation, the photogenerated electrons are transferred to Ag nano-core as the two systems undergo charge equilibration. The transfer of electrons from the excited semiconductor to the metal is an important aspect that dictates the overall energetics of the composite and hence the efficiency of photocatalytic reduction process.[17,45−47]

To confirm the participation of TiO_2 shell in transferring electrons to Ag core, we compared the photoresponse with that of Ag@SiO_2 particles. When the UV-irradiation experiments were repeated with the Ag@SiO_2 colloids in deaerated ethanol, we fail to see any changes in the plasmon absorption (Figure 2B). The plasmon absorption band with a maximum at 410 nm remained unperturbed during the UV-irradiation. By comparing the experimental results in Figure 2, parts A and B, we can conclude that the changes in the absorption seen in Ag@TiO_2 arise from the UV excitation of the shell and not the silver core. The photoactive TiO_2 shell thus, plays an important role of absorbing incident photons and injecting electrons into the silver core. The processes that lead to storing of electrons in the Ag core are summarized below (reactions 3−5).

$$TiO_2 \rightarrow TiO_2(e + h) \quad (3)$$

$$TiO_2(h) + \text{ethanol} \rightarrow \text{products} \quad (4)$$

$$TiO_2(e) + Ag \rightarrow TiO_2 + Ag(e) \quad (5)$$

The photoactivity of TiO_2 colloids was separately checked by carrying out UV-irradiation of TiO_2 colloids in deaerated ethanol. Under UV excitation, TiO_2 undergoes charge separation (reaction 1) followed by charge recombination and interfacial charge-transfer processes. As the photogenerated holes are scavenged by ethanol, the electrons accumulate within the TiO_2 particles. The electron storage in TiO_2 particles is marked by the blue coloration with characteristic broad absorption in the red region (Figure 2C). As shown earlier,[17,48] this absorption arises from electron trapping at Ti^{4+} sites. The trapped electrons are long-lived in N_2 purged suspensions and are readily extracted when needed, e.g., by transfer of electrons to acceptor molecules such as thionine or C_{60}. Since metal particles such as silver and gold with a favorable Fermi level (E_F =0.4 V) are good electron acceptors, we expect a facile electron transfer from excited TiO_2. This property of charge equilibration between semiconductor and metal nanoparticles has been independently confirmed by the addition of metal colloids to preirradiated TiO_2 colloids in ethanol.[16,17] The disappearance of the blue coloration (or absorbance at 600 nm) in this study has been used to determine the quantitative transfer of electrons to metal particles. The spectra recorded in Figure 2A do not indicate absorption in the red-IR region similar to the increase observed in Figure 2C. The lack of blue coloration in UV-irradiated Ag@TiO_2 colloids indicates that the electrons fail to accumulate in the TiO_2 shell, instead they are transferred to the silver core. The only spectral change we observe in this system is the shift in the plasmon absorption arising from the electron accumulation in the metal core.

When the UV-excitation of Ag@TiO_2 is carried out in the presence of an electron acceptor such as thionine dye or oxygen, we do not observe any shift in the plasmon absorption of silver core. As the photogenerated electrons are scavenged by the acceptor molecules, electrons fail to accumulate in the Ag core. These observations parallel the results reported for Ag/ZnO[47] and Au@SnO_2[39] nanoclusters and ascertain the argument that the shift in the plasmon absorption arises from electron storage in the Ag core.

We checked the reproducibility of charging and discharging of Ag@TiO_2 system by repeated cycles of UV-irradiation of deaerated suspension followed by exposure to air. Figure 3 show the reproducibility of plasmon absorption peak response to the UV-irradiation and air exposure in dark. The plasmon absorption band shifts from 470 to 420 nm during 1 min UV irradiation of deaerated Ag@TiO_2 suspension. The plasmon absorption regains the original spectral features when the stored electrons are

(44) Templeton, A. C.; Pietron, J. J.; Murray, R. W.; Mulvaney, P. *J. Phys. Chem. B* **2000**, *104*, 564
(45) Shanghavi, B.; Kamat, P. V. *J. Phys. Chem. B* **1997**, *101*, 7675.
(46) Subramanian, V.; Wolf, E. E.; Kamat, P. V. *J. Phys. Chem. B* **2003**, *107*, 7479.
(47) Wood, A.; Giersig, M.; Mulvaney, P. *J. Phys. Chem. B* **2001**, *105*, 8810.
(48) Kamat, P. V.; Bedja, I.; Hotchandani, S. *J. Phys. Chem.* **1994**, *98*, 9137.

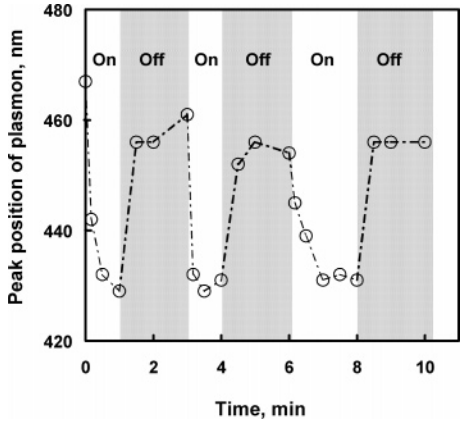

Figure 3. Response of plasmon absorbance peak to electron storage following the UV-irradiation of deaerated Ag@TiO_2 colloidal suspension in ethanol and dark discharge in air.

discharged in dark by exposing to air. We can repeat the photoinduced charging and dark discharge cycles repeatedly and reproduce the plasmon absorption response to stored electrons (Figure 3). The suspension was deaerated for 20 min before UV irradiation of each charging cycle. No such absorption changes in the plasmon absorption are seen for Ag@SiO_2 system under similar experimental conditions.

A similar but less pronounced effect was noted for Au capped with SnO_2 particles.[39] The electrons were injected chemically using a reductant, $NaBH_4$. The electrons injected into SnO_2 are transferred to Au core until the two systems attain equilibration. However, the dark discharge of electrons takes several hours to take into effect. This is attributed to the fact that the conduction band of SnO_2 is around 0 V versus NHE and is slightly more positive than oxygen reduction potential. On the other hand TiO_2 conduction band is around -0.5 V vs NHE at pH 7 and is energetically capable of transferring electrons to O_2. It should be noted that both the semiconductor shell and the metal core undergo Fermi level equilibration to attain an energy level close to the conduction band of the semiconductor. In the presence of a redox couple the composite system further attains equilibration by transferring excess charges into the acceptor molecules. By comparing the discharge response of Ag@TiO_2 and Au@SnO_2 to oxygen, we can conclude that Ag@TiO_2 clusters are energetically superior catalyst for promoting reduction process.

Estimation of Electrons Stored in Ag Core. Since the electrons stored in the Ag@TIO_2 colloids can equilibrate with the redox couple in solution, it is possible to carry out a redox titration and obtain quantitative information on the stored electrons. The dye thionine with absorption at 600 nm (ϵ = 60 000 M^{-1} cm^{-1}) is a good electron acceptor that initially produces a one electron reduction product, semithionine (Reaction 6). The semithionine ($TH^{\bullet -}$) immediately disproportionates to produce a two electron reduction product, leuco dye (TH^{2-}), with no absorption in the visible (reaction 7).

$$2TH + Ag@TiO_2(2e^-) \rightarrow 2TH^{\bullet -} + Ag@TiO_2 \qquad (6)$$

$$2TH^{\bullet -} \rightarrow TH + TH^{2-} \qquad (7)$$

The disappearance of one thionine molecule thus, represents transfer of two electrons. The reduction of thionine thus serves as the basis for titrating electrons stored in the Ag@TiO_2 clusters.

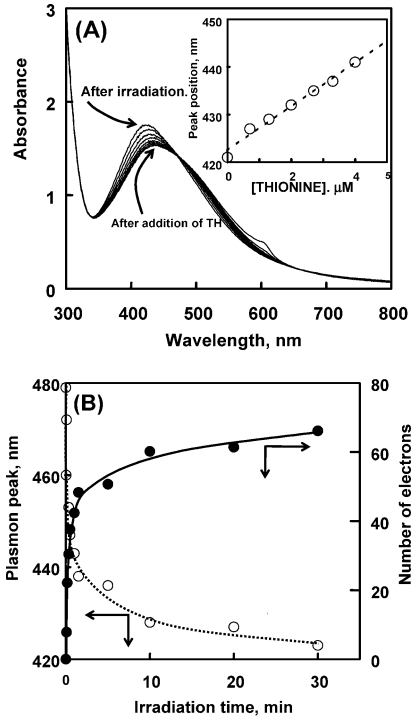

Figure 4. (A) Controlled discharge of stored electrons from Ag@TiO_2 suspension (pre-UV-irradiated under deaerated conditions) using known amounts of thionine dye. Inset shows the plasmon absorption peak position with increasing concentration of thionine. (B) Dependence of plasmon absorption peak and number of stored electrons on the time of UV-irradiation. (The number of stored electrons was calculated by titrating with thionine dye)

Known amounts of concentrated thionine solution (degassed) was injected in small increments into the UV-irradiated Ag@TiO_2 suspension. The absorption spectrum was recorded after each addition of thionine. Since the reduced dye does not have any absorption in the visible, we only observe a shift in the plasmon absorption band as the electrons are titrated using thionine. The process of electron transfer to the dye molecules continues until most of the stored electrons are discharged. The presence of any unreduced thionine is marked by the appearance of 600 nm absorption band. The endpoint of titration is thus attained when we observe the appearance of the 600 nm band. Figure 4A shows the changes in the absorption spectrum following the addition of thionine. The plasmon absorption shift and stored electrons were estimated at different irradiation times by titration of the stored electrons with thionine. The dependence of the plasmon shift and the number of stored electrons versus the UV-irradiation time is shown in Figure 4B. Saturation in electron storage is seen as we extend the UV-irradiation for a longer time.

As discussed in the earlier section, we observe a red-shift in the plasmon absorption band with increased addition of thionine to UV-irradiated Ag@SiO_2 suspension. After attaining the endpoint a small peak corresponding to thionine at 600 nm is seen. The plasmon shift corresponding to the discharge of the stored electrons in the Ag@TiO_2 cluster can thus be related to the concentration of thionine added to discharge the electrons (inset, Figure 4A). From the slope of this linear plot, we estimate that 0.42 μM electrons cause 1 nm shift in the plasmon absorption in a 2.1×10^{17} particles/liter Ag@TiO_2 suspension.

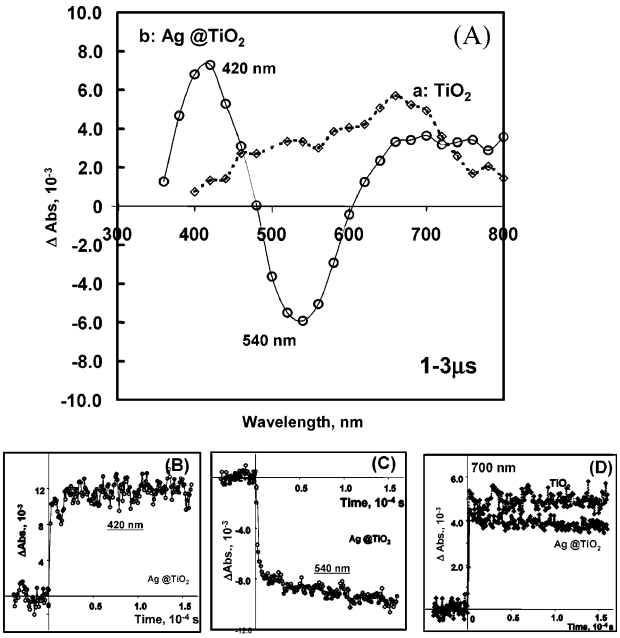

Figure 5. (A) Difference absorption spectra of deaerated colloidal Ag@TiO_2 (○) and TiO_2 (◇) suspension recorded following 308 nm laser pulse excitation. (B) Representative absorption−time profiles at 420 nm. (C) 540 nm and (D) 700 nm (experimental conditions are the same as in Figure 5A).

On the basis of the net shift observed in the plasmon band, we expect a maximum storage of about 66 electrons per Ag@TiO_2 core@shell particle. The ability of Ag@TiO_2 to store large number of electrons during UV-irradiation shows the importance of such composite structures in light energy conversion by storing electrons during photoirradiation and delivering these electrons on demand. The capacity of electron storage is determined by the size of the metal core and its ability to undergo charge equilibration with the TiO_2 shell. Once this maximum storage limit is attained, electron−hole recombination in the TiO_2 shell dominates.

Transient Absorption Studies using Laser Flash Photolysis. The photoinduced charge-transfer events were probed using nanosecond laser flash photolysis. The transient absorption spectra recorded following 308 nm laser pulse excitation of deaerated colloidal TiO_2 and Ag@TiO_2 suspension are shown in Figure 5 (A). The spectra were recorded 1 μs after laser pulse excitation. The TiO_2 colloids exhibit broad absorption in the 400−800 nm region corresponding to the trapping of electrons at Ti^{4+} sites. The Ti^{3+} centers formed as a result of electron trapping have been characterized in earlier studies.[49−52] The Ag@TiO_2 clusters exhibit strong bleaching in the plasmon absorption region in addition to the absorption in the red. The absorption band at 420 nm and bleaching at 540 nm is the result of shift in the plasmon band following the electron storage. It is interesting to note that the spectral feature of the transient spectrum (spectrum b in Figure 5A closely match the difference

Scheme 3

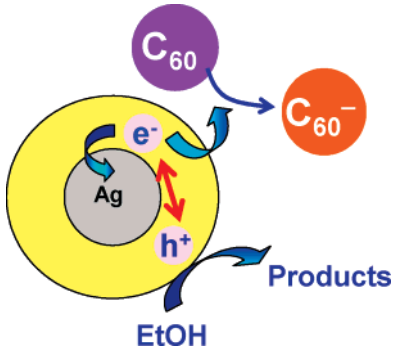

spectrum recorded in steady-state photolysis as shown in the inset of Figure 2A. This observation indicates that the absorption change observed in steady-state photolysis is a spontaneous process that follows the excitation of the TiO_2 shell. The transient absorption−time profile (Figure 5B) shows that most of the charge transfer from excited TiO_2 to Ag is completed within the laser pulse duration of few nanoseconds. A slow growth that contributes about 10% of the signal arises from the charge equilibration process which extends up to 150 μs (Figure 5C). The absorption in the red region shows the residual electrons trapped within the TiO_2 nanoparticles. These are excess trapped electrons that survive within the TiO_2 shell following charge equilibration. Figure 5D compares the transient absorption profiles at 700 nm. The maximum absorbance at 700 nm is lower for Ag@TiO_2 than the TiO_2 colloids as a fraction of the electrons are transferred to Ag core immediately following the laser pulse excitation.

Photocatalytic Activity of Ag@TiO_2 Particles. We compared the photocatalytic activity of the Ag@TiO_2 with that of TiO_2 colloids by carrying out reduction of C_{60} following 308 nm laser pulse excitation (Scheme 3). In our earlier studies, we have shown that C_{60} is an excellent probe to study the interfacial electron transfer in colloidal semiconductor systems.[53] The formation of $C_{60}^{\bullet-}$ with characteristic absorption in the IR region (1075 nm) can be conveniently used to obtain quantitative information on the electron-transfer yield. Figure 6(A) shows the difference absorbance spectrum obtained after 308 nm laser pulse excitation of Ag@TiO_2 colloids in the presence of C_{60}, The absorption maximum at 1075 nm indicates formation of C_{60} anion, $C_{60}^{\bullet-}$, as the excited Ag@TiO_2 transfer electrons to C_{60}. As can be seen from the inset of Figure 6A the C_{60}^{-} formation is completed in 100μs. The slow formation of $C_{60}^{\bullet-}$ is the indication of the time required to attain charge equilibration between C_{60} and Ag@TiO_2 system (Since C_{60} also absorbs at the excitation wavelength, we observe triplet C_{60} formation (absorption maximum at 740 nm) along with the $C_{60}^{\bullet-}$ formation. The excited C_{60} is practically inert under present experimental conditions as it does not interact with the TiO_2 surface.)

The maximum absorbance recorded 100 μs after laser pulse excitation was used to determine the relative yield of electron-transfer process in TiO_2 and Ag@TiO_2 colloids. Figure 6B shows the photocatalytic reduction yield as a function of the concentration of added C_{60} for the two systems. The electron transfer yield increased initially with increasing concentration of C_{60} and reaching a plateau at C_{60} concentration >30 μM.

(49) Gopidas, K. R.; Bohorquez, M.; Kamat, P. V. *J. Phys. Chem.* **1990**, *94*, 6435.
(50) Bahnemann, D.; Henglein, A.; Lilie, J.; Spanhel, L. *J. Phys. Chem.* **1984**, *88*, 709.
(51) Howe, R. F.; Graetzel, M. *J. Phys. Chem.* **1985**, *89*, 4495.
(52) Rajh, T.; Ostafin, A. E.; Micic, O. I.; Tiede, D. M.; Thurnauer, M. C. *J. Phys. Chem.* **1996**, *100*, 4538.
(53) Kamat, P. V.; Gevaert, M.; Vinodgopal, K. *J. Phys. Chem. B* **1997**, *101*, 4422.

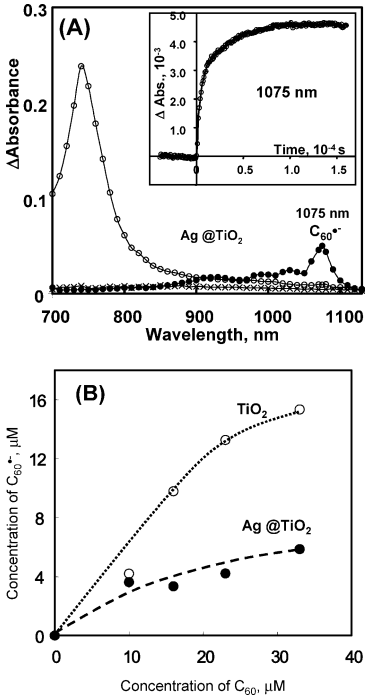

Figure 6. (A) Difference absorption spectra recorded 0.1 μs (○) and 15 μs (●) after 308 nm laser pulse excitation of deaerated Ag@TiO_2 colloidal suspension in ethanol containing 32 μM C_{60}. Inset shows the growth of $C_{60}^{\bullet-}$ as monitored from the absorption at 1075 nm. (B) Yield of $C_{60}^{\bullet-}$ (as monitored from the absorbance at 1075 nm, ϵ=16000$M^{-1}cm^{-1}$) with increasing concentration of C_{60} present in colloidal Ag@TiO_2 suspension (deaerated with N_2, Ex., 308 nm).

The electron transfer from excited TiO_2 and Ag@TiO_2 to C_{60} proceeds until the two systems attain redox equilibration. Although we expected to see a higher catalytic activity for the Ag@TiO_2 clusters, the experimental results show an opposite trend. The photocatalytic reduction efficiency of Ag@TiO_2 is lower than that of TiO_2. These results suggest that part of the photogenerated electrons reside within the Ag@TiO_2 composite as it attains equilibration with $C_{60}^{\bullet-}$.

In our earlier study of Au−TiO_2 sandwich structure (i.e., two particles in contact with each other in a coupled geometry), we observed a higher catalytic activity compared to TiO_2. The increased photocatalytic reduction was attributed to the shift of Fermi level to more negative potentials. Since $C_{60}/C_{60}^{\bullet-}$ couple equilibrates with the stored charges within the composite, the yield of $C_{60}^{\bullet-}$ serves as a measure of the apparent Fermi-level. The lower yield of $C_{60}^{\bullet-}$ observed in the present experiments suggests that the apparent Fermi-level of the Ag@TiO_2 composite is lower than TiO_2 alone. The charge equilibration between the metal core and semiconductor shell, thus causes the apparent Fermi-level less negative than neat TiO_2 cluster. Although metal core-semiconductor shell structures are quite efficient for storing photogenerated electrons, there ability to catalyze a reduction process is limited. The results presented here highlight the importance of designing semiconductor-metal composite nanostructures for light energy harvesting applications.

Conclusions

We have demonstrated the photoinduced charging and dark discharging of electrons in a silver core-semiconductor shell structure. The shift in surface plasmon band serves as a measure to determine the number of electrons stored in the metal core. The charge equilibration between the metal and semiconductor plays an important role in dictating the overall energetics of the composite. These metal core-semiconductor shell composite clusters are photocatalytically active and are useful to promote light induced electron-transfer reactions. Exploring the catalytic activity of such composite structures could pave the way for designing novel light harvesting systems.

Acknowledgment. The research described here was supported by the Office of Basic Energy Science of the U.S. Department of Energy. This is contribution number NDRL 4574 from the Notre Dame Radiation Laboratory.

JA042925A